BMC Medical Imaging

RESEARCH

Open Access

Magnetic resonance cholangiopancreatography at 5.0 T: quantitative and qualitative comparison with 3.0 T

Liang Yin[1], ZhangZhu Li[1], MingYan Shang[1], ZongChang Li[1], BoWen Tang[1], Dan Yu[2] and Jie Gan[1*]

Abstract

Background This study aimed to assess the feasibility and performance of 5.0 T MRI in MR Cholangiopancreatography (MRCP) imaging compared to 3.0 T, focusing on detail visualization, signal-to-noise ratio (SNR), and image artifacts.

Methods A prospective study from May to October 2023 involved 20 healthy subjects and 19 with biliary dilation. Both groups underwent MRCP using 3.0 T and 5.0 T scanners. The detail visualization capability of the biliary tree and the SNR of the images were quantitatively evaluated. Two experienced MRI diagnostic physicians assessed the image artifacts qualitatively on a scale of 1 to 5. The t-test or Wilcoxon signed-rank test compared the quantitative results of biliary visualization and SNR between 3.0 T and 5.0 T scanners, while the Wilcoxon signed-rank test was used for comparing the level of image artifacts between the two scanners. The inter reader consistency was tested using Kappa test.

Results In both healthy subjects and those with biliary dilation, the 5.0 T group exhibited significantly higher numbers of biliary tree branches, along with greater total and maximum branch lengths, compared to the 3.0 T group ($P<0.05$). Although the maximum branch length was higher in the 5.0 T group among healthy subjects, this difference was not statistically significant ($P=0.053$). No notable differences were observed in SNR and image artifact levels between the two groups across both field strengths ($P>0.05$).

Conclusions MRCP at 5.0 T offers superior biliary tree visualization compared to 3.0 T. The performance regarding SNR and image artifacts between the two is relatively comparable.

Keywords Ultra-high field MRI, 5.0 T, MR Cholangiopancreatography, Quantitative and qualitative comparison, Biliary tree visualization

*Correspondence:
Jie Gan
ganjie000@sina.com
[1]Department of Medical Imaging, Shandong Provincial Third Hospital, Jinan, China
[2]United Imaging Research Institute of Intelligent Imaging, Beijing, China

Background

Magnetic resonance cholangiopancreatography (MRCP), a noninvasive diagnostic tool for visualizing bile and pancreatic ducts, has advanced significantly over the past three decades [1–3]. Benefiting from advancements in MRI hardware and imaging sequences, MRCP is radiation-free and doesn't require contrast agents. It has reached a diagnostic performance on par with the gold standard, ERCP [4], making it the preferred choice for diagnosing biliary tract diseases [5–7]. Despite this progress, MRCP's effectiveness at different magnetic field strengths, particularly at ultra-high fields, remains a subject of ongoing research.

Currently, MRCP predominantly utilizes 1.5 or 3.0 T magnetic fields, employing T2-weighted (T2W) sequences that leverage the prolonged T2 relaxation times of static or slowly flowing fluids, using a respiratory-triggered 3D fast spin-echo technique [8]. The potential benefits of higher magnetic fields, such as improved signal-to-noise ratio (SNR), better spatial resolution, and enhanced tissue contrast, have sparked interest in using MRI at fields greater than 3.0 T [9–11]. Initial studies in ultra-high-field body MRI, particularly at 7.0 T, have shown promising results for abdominal imaging. For example, non-enhanced 3D FLASH imaging at 7.0 T demonstrated superior contrast and more detailed visualization of mesentery structures [12]. Additionally, a study with ten healthy volunteers highlighted the effectiveness of 7.0 T 3D FLASH in rapidly acquiring high-quality, non-enhanced images of renal vasculature [13].

Abdominal imaging with 7.0 T MRI faces several challenges [14]. The ultra-high field strength leads to uneven distribution of the RF field (B1), adversely impacting image quality due to the inhomogeneous B1 field. This results in more artifacts and lower image quality in 7.0 T MRI compared to 1.5 and 3.0 T [15]. Specifically, for biliary tract imaging, the T2W turbo spin-echo sequence at 7.0 T struggles with B1 field inhomogeneities, compromising image quality [16]. Similar challenges are observed in renal MRI at 7.0 T, as noted by Umutlu et al., where image quality is significantly affected [17].

Recent developments in 5.0 T MRI technology offer potential advantages for abdominal MRCP imaging, presenting a promising alternative to 7.0 T MRI [18]. Theoretically, 5.0 T MRI could provide images with higher SNR than 3.0 T MRI, while better managing image artifacts compared to 7.0 T MRI [19]. This increase in SNR might enhance biliary tree visualization. However, the specific advantages of 5.0 T MRI in MRCP remain to be fully understood. Therefore, this study aimed to assess the feasibility and efficacy of 5.0 T MRI for abdominal MRCP, comparing it quantitatively and qualitatively to 3.0 T MRI in aspects like detail visualization, SNR, image quality, and artifacts.

Table 1 3D MRCP protocols parameters at 3.0 T and 5.0 T

Parameters	Sequences with Respiratory triggered	
	3.0 T	5.0 T
TR(ms)	Shortest(367 ~ 2645)	~ 4095*
TE(ms)	600	697
FA(°)	90	90
FOV(mm^2)	320 × 320	320 × 320
Matrix	300 × 300	300 × 300
Number of slices	60	60
Reconstruction Voxel volume(mm)	1 × 1 × 1.5	1 × 1 × 1.5
NEX	1	1
Acquisition time(s)	202–252	196–238

Abbreviations: 3D,3-dimensional; MRCP, magnetic resonance cholangiopancreatography; TR, repetition time; TE, echo time; FA, flip angle; FOV, field of view; NEX, number of excitation. *TR depends on the respiratory interval of participants

Methods

Patients

This prospective study was approved by the Ethics Committee of Shandong Provincial Third Hospital (KYLL-2023064). All participants were informed about the study and provided written informed consent. From May to October 2023, a total of 40 participants were recruited, including healthy volunteers and volunteers with bile duct dilation caused by bile duct stones from the hospital's outpatient population. Inclusion criteria were as follows: (a) age > 18 years with capacity for autonomous decision-making; (b) no contraindications for MRI examination (e.g., presence of cardiac pacemaker, history of neurological or psychiatric disorders, metal implants). Exclusion criteria were: (a) a history of abdominal surgery; (b) a history of biliary stent placement; (c) liver disease; (d) significant abdominal ascites; (e) a history of biliary tract tumors. Each volunteer underwent a 3D MRCP examination within 24 h, using 3.0 T and 5.0 T scanners, respectively.

MRI acquisitions

All participants underwent a minimum of 6 h of fasting prior to the examination. The 5.0 T MRI scan was conducted using the state-of-the-art ultra high field MRI system (uMR Jupiter, United Imaging Healthcare) equipped with a 24-channel body coil and a 48-channel spine coil. However, only 16-channel body coil and 16-channel spine coil were activated during scanning. Additionally, 3.0 T MRI scans were performed on the advanced MRI system (Ingenia, Philips Healthcare) utilizing a 16-channel body coil and a 16-channel spine coil. Respiratory triggering was employed to acquire long-echo heavy T2W sequences with fat suppression. A comprehensive description of the MR protocols is provided in Table 1. The source images obtained through the 3D TSE

sequence were reconstructed using a maximum intensity projection (MIP) technique.

Quantitative image analysis

Quantitative Image Analysis involved evaluating the bile duct tree branches in MRCP using a semi-automatic approach to compare visualization capabilities at two different field strengths. MIP images were reconstructed from multiple directions to ensure comprehensive visualization of the biliary tree. For quantitative analysis, the coronal MIP image orientation was selected for consistency. The process, depicted in Fig. 1, included: converting the MRCP image to an 8-bit format while excluding the gallbladder region; applying skeletonization to the image; removing disconnected parts not linked to the main bile duct trunk; calculating the longest branch; and determining the branch count, total and maximum branch lengths of the skeletonized tree. ImageJ (1.53T, https://imagej.nih.gov/ij/) [20] was used for data process ing. Specific terms used in the analysis are defined as follows: Longest Branch: The longest continuous path from the main duct to the farthest visible branch within the biliary tree. Branch Count: The total number of branches identified, encompassing primary, secondary, and any further branches within the skeletonized tree. Total Branch Length: The cumulative length of all branches in the skeletonized biliary tree. Maximum Branch Length: The length of the longest individual branch from the biliary tree root to the tip.

Additionally, identically-sized regions of interest (ROIs) of 0.2 cm diameter were placed on the bile duct's upper segment (at the level of the gallbladder duct opening), the proximal left and right hepatic ducts for signal intensity (SI) measurement. Quantitative analysis included primary and secondary branches of the bile duct tree, with ROIs placed on the 3D TSE source images for consistency in SNR calculation. The standard deviation (SD) of the background was measured around each ROI, free of artifacts and with the same diameter. SNRs for each ROI were calculated, and the final SNR_{mean} of the images was determined as the mean SNR of these three ROIs. A radiologist (L.Y.) with 11 years of abdominal MR scan experience performed all measurements.

Qualitative image analysis

Bile duct visibility was qualitatively assessed using a skeletonized tree representation, capturing the branching structure's visibility in detail. Two radiologists, L.L. (with 12 years of experience) and M.S. (with 9 years of experience), independently assessed the MRI images, blind to the acquisition technique and field strength. To minimize potential bias, the order of subjects was randomized, and 3T and 5T images were evaluated separately. Observers were allowed to adjust image contrast freely during the qualitative assessment, enabling individualized optimization for evaluating image clarity and artifact presence. They evaluated image artifacts including magnetic field inhomogeneity, chemical shift, distortion, and motion artifacts on a 5-point scale: 5 indicating severe

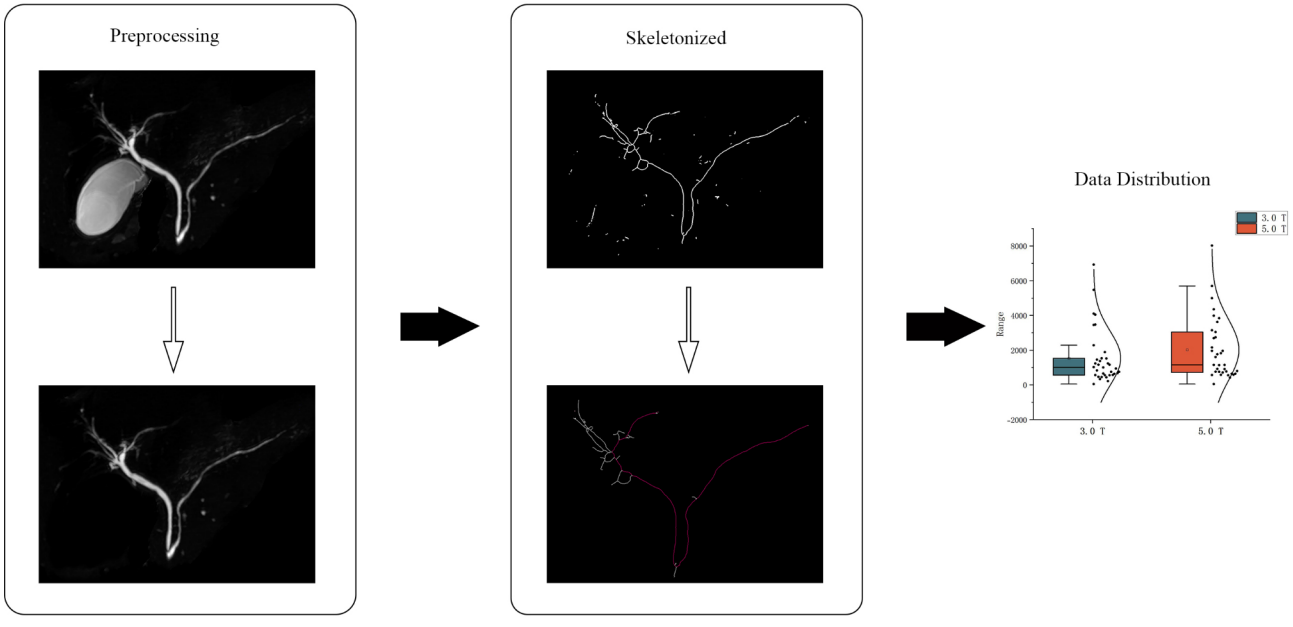

Fig. 1 Flow chart for semi-automatic quantitative analysis of maximum branch length of the biliary tree. The red line represents the identified maximum branch length; the common bile duct and main pancreatic duct, when indistinguishable in the MIP image, will be collectively recognized as the maximum branch length, occurring at both 3T and 5T

impairment rendering the images non-diagnostic; 4 indicating strong impairment; 3 indicating moderate impairment; 2 indicating slight impairment; and 1 indicating no impairment.

Statistical analysis

The *S*hapiro-*W*ilk test assessed data normality. For data that was normally distributed, means and standard deviations were calculated. Conversely, for non-normally distributed data, medians and interquartile ranges were determined. The paired sample t-test were applied to normally distributed data, while *W*ilcoxon signed-rank tests were used for comparing SNR and quantitative measures at 3.0 T and 5.0 T in skewed distributions. The *K*appa consistency test assessed the agreement level between the two radiologists in qualitative analysis, with values ranging from 0 to 0.2 indicating slight agreement, 0.21 to 0.4 indicating fair agreement, 0.41 to 0.60 indicating moderate agreement, 0.61 to 0.8 indicating substantial agreement, and values above 0.8 indicating excellent agreement. Lastly, the Wilcoxon signed-rank test compared the image artifact scores at 3.0 T and 5.0 T. All statistical procedures were executed using SPSS (version 26.0), and a $P<0.05$ was considered indicative of statistical significance."

Results

Subjects

Throughout the study, 21 healthy individuals and 19 patients with bile duct dilation were subjected to MRCP examinations. However, one healthy participant was excluded due to claustrophobia during the 3.0 T scan. Consequently, the study included 20 healthy subjects (9 females and 11 males, average age 33.2±9.9 years) and 19 patients with bile duct dilation (7 females and 12 males, average age 57.3±12.4 years). The patients with bile duct dilation had diagnoses of common bile duct stones ($n=12$) or hilar bile duct stones ($n=7$), confirmed by ultrasound or CT.

Visualization and quantitative assessment of the bile duct tree

In this study, the healthy volunteer group exhibited higher branch counts, total branch lengths, and maximum branch lengths in the biliary tree on 5.0 T MRCP images compared to 3.0 T, as detailed in Table 2. The differences in branch count and total branch length were statistically significant ($P<0.05$), while the difference in maximum branch length was not ($P=0.053$). Similarly, for the group with biliary dilation, 5.0 T MRCP images showed significantly higher branch count, total branch length, and maximum branch length compared to 3.0 T ($P<0.05$), as indicated in Table 2. Figures 2 and 3 display comparative biliary tree images of volunteers with choledocholithiasis-induced intrahepatic and extrahepatic biliary dilation at both 3.0 T and 5.0 T.

Quantitative assessment of SNR

For the group with bile duct dilation, the SNRs for the 3.0 T and 5.0 T groups were recorded as 77.51±25.68 and 91.24±23.08, respectively. In the healthy group, the SNR values at 3.0 T and 5.0 T were 69.53±30.68 and 80.75±25.11, respectively. The difference in SNR between the two groups was not statistically significant ($P>0.05$), as indicated in Table 3.

Analysis of image artifacts

Subjective evaluations of 3D MRCP pseudobleaching under the two field strengths were conducted, with results presented in Table 4. The assessment showed excellent observer consistency in subjective image observations. There was no significant difference in pseudobleaching scores between the 5.0 T and 3.0 T images ($P=0.053$).

Discussion

Enhanced detail resolution in MRCP images offers clearer and more precise visualization of anatomical variations in bile ducts, particularly useful for patients with bile duct calculus [21]. These images provide critical

Table 2 Quantitative image analysis for MRCP imaging at 3.0 T and 5.0 T

Equipment	The biliary tree of the dilated bile duct group			The biliary tree of the healthy group		
	number of branches (pixel)	total branch length (pixel)	maximum branch length (pixel)	number of branches (piece)	total branch length (pixel)	maximum branch length (pixel)
3.0 T	31.00(18.00, 63.00)	1534.05(1008.09, 3474.38)	230.27±80.20	11.45±4.08	572.34(441.18, 1131.72)	196.17(149.22, 259.84)
5.0 T	35.00(22.00, 66.00)	3045.30(1765.33, 4065.70)	275.06±83.50	12.80±5.01	737.66(584.49, 1095.86)	220.06(187.60, 262.65)
Statistical value	-3.585[b]	-3.139[b]	-3.802[a]	-2.969[a]	-2.875[b]	-2.128[b]
P	<0.001	0.002	0.001	0.008	0.004	0.053

Normal distribution data is expressed as Mean±SD, while non-normal distribution data is represented by median and interquartile range. [a] is *t* value from the paired sample t-test; [b] is the *Z* value from the Wilcoxon signed-rank tests

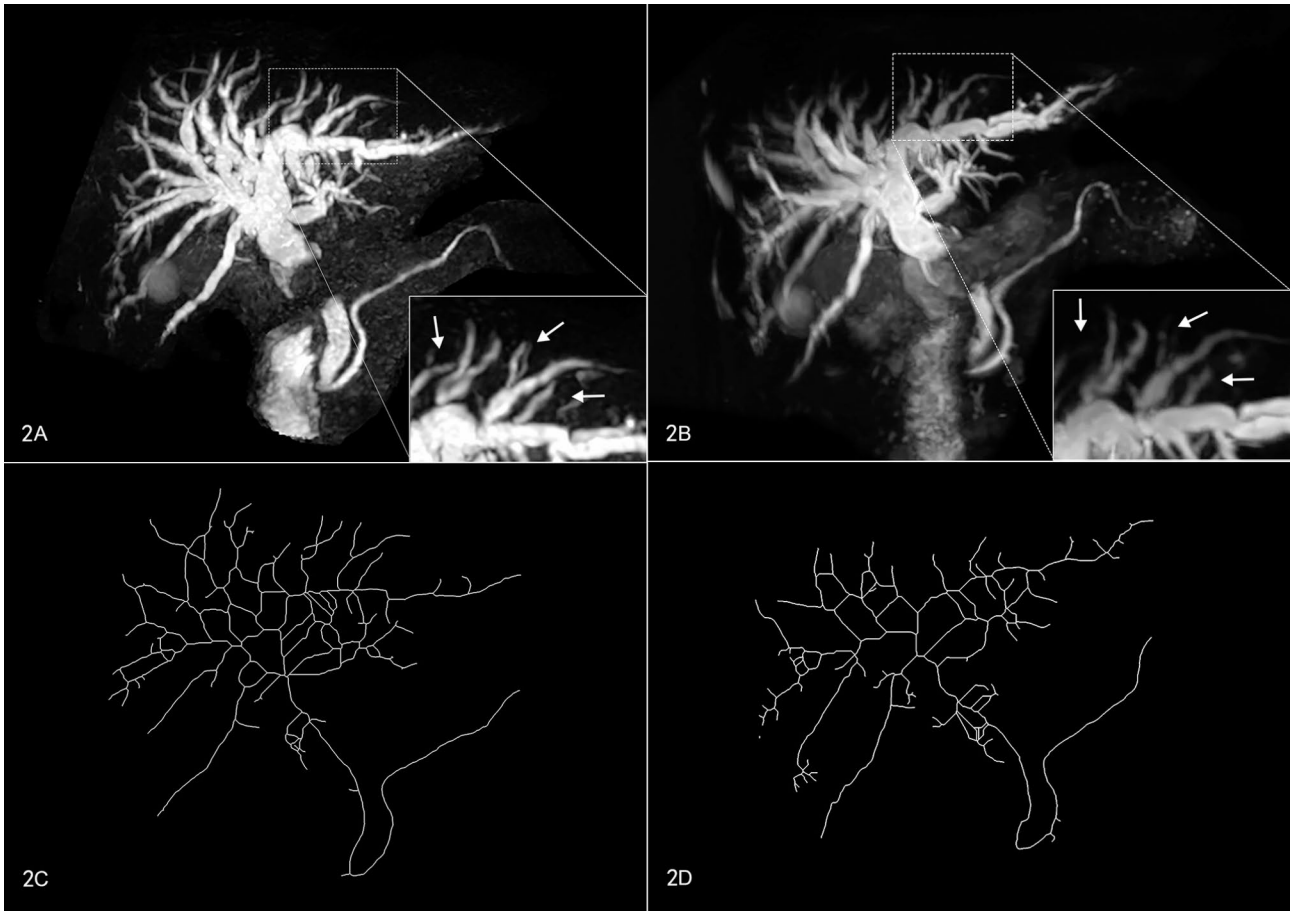

Fig. 2 Taken from a subject with dilated bile ducts due to common bile duct stones, the MIP image of 5.0 T (A) demonstrates more detail of the bile duct tree (white arrows) than 3.0 T (B). C and D are skeletonized views of the dilated biliary tree at 5.0 T and 3.0 T

information on the location, size, and number of calculi, aiding in clinical decision-making. In this study, a semi-automated quantitative approach was used to compare bile duct branch visualization in 3.0 T and 5.0 T MRCP images. Cross-validation revealed that 5.0 T MRCP provided superior anatomical detail, especially in cases with bile duct dilation, exhibiting significantly better branch quantity, total length, and maximum length.

The signal intensity of the same tissue exhibits a positive correlation with the B0 field strength, allowing higher field strength MRI to yield images with increased SNR [22]. Previous studies confirm this, showing improved differentiation of choledochal and periductal tissues, as well as overall image quality, when upgrading the MRI device's B0 field from 1.5 T to 3.0 T [23].

The contrast in MR images at different magnetic field strengths is influenced by variations in the T1 and T2 relaxation times of each organ or tissue. Generally, T1 relaxation times are longer and T2 relaxation times shorter at 5.0 T than at 3.0 T, but this varies across different tissues [24]. While our images showed a tendency for higher SNR at 5.0 T compared to 3.0 T, this disparity was not statistically significant ($P>0.05$). This contrasts with a recent 5.0 T MRI study of the pancreas involving 18 healthy volunteers, which showed superior SNR and satisfactory image quality in T2W and diffusion-weighted imaging at 5.0 T compared to 3.0 T [25]. MRCP imaging, based on the long T2 relaxation time of fluid in the biliopancreatic ducts, opts for fast acquisition of relaxation-enhanced sequences for heavy T2W imaging, making it more susceptible to B1-field inhomogeneity than normal abdominal organ imaging [3, 26]. Additionally, B1 field inhomogeneity amplifies image noise [27], reducing liquid signal strength when scanning protocols are optimized for background noise.

Although 5.0 T MRI has shown advantages of high SNR in cranial and cardiovascular imaging compared to 3.0 T [19, 28, 29], further studies in abdominal imaging are necessary to confirm its potential. Zheng L et al. found significantly better image quality of renal veins and arteries with comparable artifact levels in T1-weighted images at 5.0 T compared to 3.0 T, and on T2W images, the image quality was similar for both field strengths, but higher artifact levels were observed at 5.0 T [30].

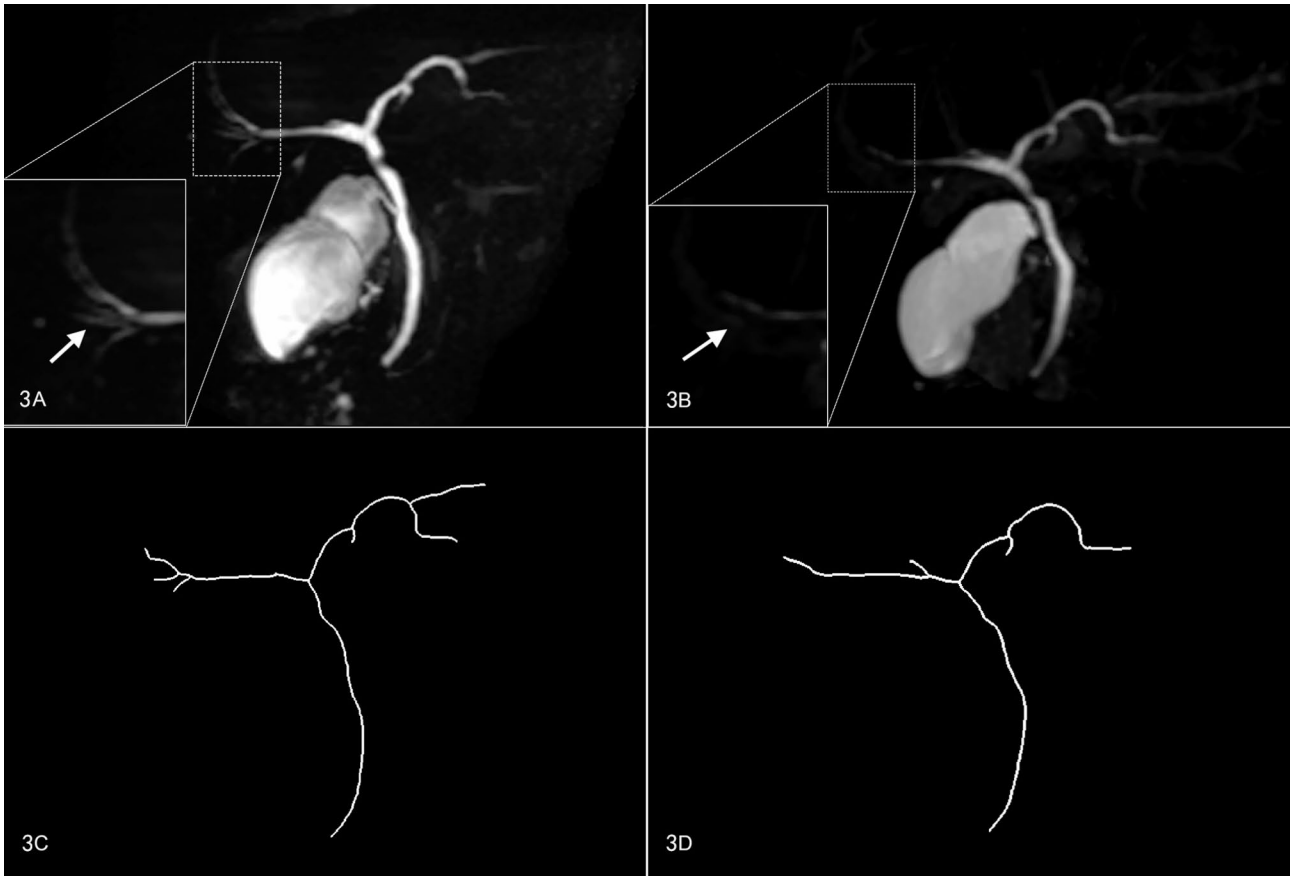

Fig. 3 A healthy subject. Intrahepatic bile duct branches in the right lobe of the liver are better visualized at 5.0 T (A) than at 3.0 T (B) (white arrow). C and D are skeletonized views of the undilated biliary tree at 5.0 T and 3.0 T, showing that 5.0 T exhibits more branches and a greater maximum branch length compared to 3.0 T

Table 3 SNR of MRCP imaging at 3.0 T and 5.0 T

Equipment	SNR of the dilated bile duct group	SNR of the healthy group
3.0T	77.51 ± 25.68	69.53 ± 30.68
5.0T	91.24 ± 23.08	80.75 ± 25.11
t value	-2.086	-1.260
P	0.052	0.223

The *t* value derives from the paired sample T-test

Scanning protocols for heavy T2W water imaging in 5.0 T MRI systems still require optimization.

With increasing field strength, the Larmor wavelength decreases, leading to noticeable B1 inhomogeneity in larger anatomical regions at 7.0 T [16]. Hence, 5.0 T may have advantages in artifact control over 7.0 T. Despite potential drawbacks associated with ultra-high fields, such as dielectric effects and susceptibility artifacts, this study shows 5.0 T is comparable to 3.0 T in artifact control, enabling whole-body scans at ultra-high fields.

There are several limitations to this study. The primary concern is the small sample size, which might affect the reliability of the results. Future studies with larger cohorts are planned to bolster the findings' credibility. Additionally, the study focused exclusively on the 3D TSE protocol triggered by respiration, omitting the 3D GRASE imaging during a single breath-hold, equally

Table 4 Score of image artifacts for MRCP imaging at 3.0 T and 5.0 T

Equipment	Observer	Score*					KAPPA	*Z*	*P*
		1	2	3	4	5			
3.0 T	A	12	18	9	0	0	0.842	-1.933	0.053
	B	12	16	11	0	0			
5.0 T	A	11	16	11	1	0	0.809		
	B	10	18	11	0	0			

*The value is the number of volunteers scoring in this category

vital for diagnosing pancreatic and biliary diseases [31]. Furthermore, the use of scanners and phased array coils from different manufacturers could introduce variability. However, this was mitigated by using identical scanning parameters and activating the same number of coil channels for all scans.

Conclusions

In summary, this study demonstrates that 5.0 T MRCP offers improved anatomical detailing of the biliary tree over 3.0 T, while maintaining comparable SNR and image artifact levels. The enhanced detail provided by 5.0T MRCP facilitates clearer visualization of biliary structures, offering a foundation for future studies on its potential in identifying small biliary stones within minor intrahepatic branches.

Abbreviations

MRI	Magnetic resonance imaging
MRCP	Magnetic resonance cholangiopancreatography
SNR	Signal-to-noise ratio
ERCP	Endoscopic retrograde cholangiopancreatography
RF	Radio-frequency
3D TSE	Three dimensional turbo spin echo
3D GRASE	Three dimensional gradientrecalled and spin echo

Acknowledgements

Not applicable.

Author contributions

All authors contributed to this paper. YL and LZZ: Writing original draft, Data collection, Data analysis. SMY: Data analysis, Visualization. LZC and TBW: MRI scanning, Data collection. YL: Statistical analysis, Conceptualization, Methodology. GJ and YD: Conceptualization, Supervision, Project administration, Writing review and editing. All authors read and approved the final manuscript.

Funding

This study was supported by Outstanding Young Talents Fund of Shandong Provincial Third Hospital (jqrc007). The funding body played no role in the design of the study and collection, analysis, interpretation of data, and in writing the manuscript.

Data availability

The datasets used and/or analyzed during the current study are available from the corresponding author on reasonable request.

Declarations

Ethics approval and consent to participate

All procedures performed in studies involving human participants were in accordance with the ethical standards of the institutional and/or national research committee and with the 1964 Helsinki declaration and its later amendments or comparable ethical standards. This prospective study was approved by the Ethics Committee of Shandong Provincial Third Hospital (KYLL-2023064). All participants were informed about the study and provided written informed consent.

Consent for publication

Not applicable.

Competing interests

The authors declare no competing interests.

Received: 4 April 2024 / Accepted: 21 November 2024

Published online: 05 December 2024

References

1. Yoen H, Lee JM, Lee SM, et al. Comparisons between image quality and diagnostic performance of 2D- and breath-hold 3D magnetic resonance cholangiopancreatography at 3T. Eur Radiol. 2021;31(11):8399–407.
2. Griffin N, Yu D, Alexander Grant L. Magnetic resonance cholangiopancreatography: pearls, pitfalls, and pathology. Semin Ultrasound CT MR. 2013;34(1):32–43.
3. Sahni VA, Mortele KJ. Magnetic resonance cholangiopancreatography: current use and future applications. Clin Gastroenterol Hepatol. 2008;6(9):967–77.
4. Hekimoglu K, Ustundag Y, Dusak A, et al. MRCP vs. ERCP in the evaluation of biliary pathologies: review of current literature. J Dig Dis. 2008;9(3):162–9.
5. Itani M, Lalwani N, Anderson MA, Arif-Tiwari H, Paspulati RM, Shetty AS. Magnetic resonance cholangiopancreatography: pitfalls in interpretation. Abdom Radiol (NY). 2023;48(1):91–105.
6. Kaltenthaler E, Vergel YB, Chilcott J et al. A systematic review and economic evaluation of magnetic resonance cholangiopancreatography compared with diagnostic endoscopic retrograde cholangiopancreatography. Health Technol Assess. 2004. 8(10): iii, 1–89.
7. Buxbaum JL, Abbas Fehmi SM, Sultan S, et al. ASGE guideline on the role of endoscopy in the evaluation and management of choledocholithiasis. Gastrointest Endosc. 2019;89(6):1075–e110515.
8. Wang K, Li X, Liu J, et al. Predicting the image quality of respiratory-gated and breath-hold 3D MRCP from the breathing curve: a prospective study. Eur Radiol. 2023;33(6):4333–43.
9. Park JE, Cheong EN, Jung DE, Shim WH, Lee JS. Utility of 7 Tesla Magnetic Resonance Imaging in patients with Epilepsy: a systematic review and Meta-analysis. Front Neurol. 2021;12:621936.
10. Giraudo C, Motyka S, Weber M, Feiweier T, Trattnig S, Bogner W. Diffusion Tensor Imaging of Healthy Skeletal Muscles: a comparison between 7 T and 3 T. Invest Radiol. 2019;54(1):48–54.
11. Lecler A, Duron L, Charlson E, et al. Comparison between 7 Tesla and 3 Tesla MRI for characterizing orbital lesions. Diagn Interv Imaging. 2022;103(9):433–9.
12. Hahnemann ML, Kraff O, Orzada S, et al. T1-Weighted contrast-enhanced magnetic resonance imaging of the small bowel: comparison between 1.5 and 7 T. Invest Radiol. 2015;50(8):539–47.
13. Umutlu L, Maderwald S, Kraff O, et al. New look at renal vasculature: 7 tesla nonenhanced T1-weighted FLASH imaging. J Magn Reson Imaging. 2012;36(3):714–21.
14. Fiedler TM, Orzada S, Flöser M, et al. Performance and safety assessment of an integrated transmit array for body imaging at 7 T under consideration of specific absorption rate, tissue temperature, and thermal dose. NMR Biomed. 2022;35(5):e4656.
15. Laader A, Beiderwellen K, Kraff O, et al. 1.5 versus 3 versus 7 Tesla in abdominal MRI: a comparative study. PLoS ONE. 2017;12(11):e0187528.
16. Fischer A, Kraff O, Orzada S, et al. Ultrahigh-field imaging of the biliary tract at 7 T: initial results of gadoxetic acid-enhanced magnetic resonance cholangiography. Invest Radiol. 2014;49(5):346–53.
17. Umutlu L, Orzada S, Kinner S, et al. Renal imaging at 7 Tesla: preliminary results. Eur Radiol. 2011;21(4):841–9.
18. Zhang Y, Yang C, Liang L, et al. Preliminary experience of 5.0 T higher field abdominal diffusion-weighted MRI: agreement of Apparent Diffusion Coefficient with 3.0 T imaging. J Magn Reson Imaging. 2022;56(4):1009–17.
19. Wei Z, Chen Q, Han S, et al. 5T magnetic resonance imaging: radio frequency hardware and initial brain imaging. Quant Imaging Med Surg. 2023;13(5):3222–40.
20. Schindelin J, Arganda-Carreras I, Frise E, et al. Fiji: an open-source platform for biological-image analysis. Nat Methods. 2012;9(7):676–82.
21. Afzalpurkar S, Giri S, Kasturi S, Ingawale S, Sundaram S. Magnetic resonance cholangiopancreatography versus endoscopic ultrasound for diagnosis of choledocholithiasis: an updated systematic review and meta-analysis. Surg Endosc. 2023;37(4):2566–73.
22. Rutland JW, Delman BN, Gill CM, Zhu C, Shrivastava RK, Balchandani P. Emerging Use of Ultra-high-field 7T MRI in the study of Intracranial Vascularity: state of the field and future directions. AJNR Am J Neuroradiol. 2020;41(1):2–9.

23. Onishi H, Kim T, Hori M, et al. MR cholangiopancreatography at 3.0 T: intraindividual comparative study with MR Cholangiopancreatography at 1.5 T for clinical patients. Invest Radiol. 2009;44(9):559–65.
24. de Bazelaire CM, Duhamel GD, Rofsky NM, Alsop DC. MR imaging relaxation times of abdominal and pelvic tissues measured in vivo at 3.0 T: preliminary results. Radiology. 2004;230(3):652–9.
25. Zheng L, Yang C, Liang L, Rao S, Dai Y, Zeng M. T2-weighted MRI and reduced-FOV diffusion-weighted imaging of the human pancreas at 5 T: a comparison study with 3 T. Med Phys. 2023;50(1):344–53.
26. Van de Moortele PF, Akgun C, Adriany G, et al. B(1) destructive interferences and spatial phase patterns at 7 T with a head transceiver array coil. Magn Reson Med. 2005;54(6):1503–18.
27. Ipek Ö. Radio-frequency coils for ultra-high field magnetic resonance. Anal Biochem. 2017;529:10–6.
28. Lin L, Liu P, Sun G, et al. Bi-ventricular assessment with cardiovascular magnetic resonance at 5 Tesla: a pilot study. Front Cardiovasc Med. 2022;9:913707.
29. Shi Z, Zhao X, Zhu S, et al. Time-of-flight intracranial MRA at 3 T versus 5 T versus 7 T: visualization of distal small cerebral arteries. Radiology. 2022;305(3):E72.
30. Zheng L, Yang C, Sheng R, Dai Y, Zeng M. Renal imaging at 5 T versus 3 T: a comparison study. Insights Imaging. 2022;13(1):155.
31. Yoshida M, Nakaura T, Inoue T, et al. Magnetic resonance cholangiopancreatography with GRASE sequence at 3.0T: does it improve image quality and acquisition time as compared with 3D TSE. Eur Radiol. 2018;28(6):2436–43.

Publisher's note